

Thermal-neutron-induced Single Event Upsets in the FPGA used in particle physics experiments

C. Yamada, E. Hamada, Y. Nakazawa, K. Ueno

Abstract—Particle physics experiments using accelerators produce large amounts of background neutrons, which adversely affect electronics. A single event upset (SEU) is an error in which a neutron incident on a semiconductor device produces charged particles, thereby changing the logic of the device. If an SEU occurs in a field programmable gate array (FPGA) used in an experiment, it can compromise the reliability of its functionality. Therefore, it is crucial to accurately assess the impact of SEU and implement preventive measures before conducting physics measurements. Fast neutrons, which can react with Si nuclei to produce charged particles, are often considered the primary cause of SEUs. However, recent attention has been directed toward the possibility that thermal neutrons, which have an energy of less than 1 eV, can also cause SEUs. To investigate SEUs caused by thermal neutrons, we placed polyethylene blocks around the fast neutron beam produced by the Tandem accelerator. The fast neutrons were degraded to become thermal neutrons, which were irradiated onto the FPGA, and we measured the SEU rate. We also measured the SEU rate by placing polyethylene blocks containing boron to absorb thermal neutrons. The irradiation dose for each neutron energy band was investigated using a plastic track detector. We successfully observed SEUs by thermal neutrons and showed that thermal neutron absorbers reduce the SEU rate.

Index Terms—thermal neutrons, single event upset (SEU), Tandem accelerator, Field-programmable gate arrays (FPGAs), particle physics experiment, COMET, Belle II

I. INTRODUCTION

In particle physics experiments, some approaches to explore physics beyond the Standard Model are high-intensity, high-luminosity, or high-energy beams. While these beams are instrumental in probing new physics, they also generate substantial radiations, which affect detectors and readout modules, particularly through neutron exposure. For example, the COMET experiment [1] at J-PARC, utilizes a muon beam generated from a proton beam to investigate muon-to-electron conversion, which is one of the undiscovered decays called charged Lepton Family number Violating (cLFV) processes. Because the muon beam used in this experiment has the world's highest intensity, it is expected to observe such a process. Additionally, the Belle II experiment [2] at KEK, employing SuperKEKB, which is the highest luminosity electron-positron collider, deeply studies flavor physics by measuring the decays of billions of bottom mesons, charm hadrons, and tau leptons. For both of these experiments, it is important

This Manuscript was submitted on May 27, 2024; date of current version May 27, 2024.; This work was supported by World Premier International Research Center Initiative (WPI), MEXT, Japan. Chiro Yamada and Kazuki Ueno are with the Department of Physics, Osaka University, Osaka 565-0871, Japan (e-mail:c-yamada@epp.phys.sci.osaka-u.ac.jp) Eitaro Hamada and Yu Nakazawa are with the Institute of Particle and Nuclear Studies, High Energy Accelerator Research Organization (KEK), Tsukuba 305-0801, Japan

to achieve large statistics, which is accomplished by using advanced high-intensity or high-luminosity beams. However, the disadvantage of these approaches is the highly radioactive environments created by the beam. They produce neutrons, gamma rays, and various other extra particles, which cause damage to electronic equipment. For neutrons, in both cases of the COMET and Belle II experiments, a tolerance to about 1×10^{12} neutrons/cm² (1 MeV equivalent), including a safety factor, is required. As seen in these examples, there are significant concerns regarding the ability of electronics to withstand harsh radiation. The damage to electronics can be categorized into two types: hard errors and soft errors. A single event upset (SEU), a type of soft errors that are temporary damage, occurs when a neutron strikes a semiconductor, causing a reaction that generates charged particles within a transistor, resulting in a bit flip. The energy bands of neutrons that can cause SEUs are fast neutrons of several MeV or more and thermal neutrons of less than 1 eV. Fast neutrons interact with Si nuclei in the semiconductor generating charged particles that can induce electron-hole pairs changing the logic state of the transistor gate, causing SEUs. In particle experiments using beams generated by advanced accelerators, it is difficult to completely shield fast neutrons, and the SEU reaction rate induced by fast neutrons is often investigated [4] and countermeasures are taken by using error correcting codes. In the case of thermal neutrons, a capture reaction with boron-10 ($^{10}\text{B} + n \rightarrow ^7\text{Li} + ^4\text{He}$) produces an alpha particle, which can similarly change the logical state. When Boron-Phosphorus Silicon Glass (BPSG) films were used as insulating films in devices, more thermal-neutron-induced SEUs were caused. However, with the shift to alternative methods to BPSG, SEUs caused by thermal neutrons have decreased [5]. Nevertheless, recent studies [6], [7] have reported that thermal neutrons can still cause SEUs in newly developed FPGAs. To address this concern, we investigated SEUs caused by thermal neutrons using an FPGA used in the readout board for the COMET experiment.

II. MEASUREMENT

We conducted SEU measurements at an accelerator facility that produces fast neutrons. By arranging polyethylene(PE) blocks, we were able to observe the effects of thermal neutrons efficiently. The numbers of thermal and fast neutrons were measured using dedicated detectors.

A. Facility

The neutron irradiation test was performed at the tandem electrostatic accelerator at Kobe University. The accelerator

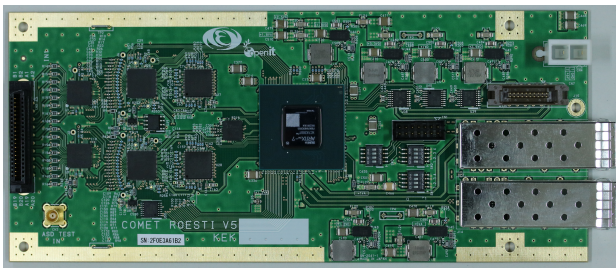


Fig. 1. Irradiated electronics board called ROESTI developed for the COMET experiment [8]. Artix-7 is placed in the center.

generates a neutron beam through the reaction (${}^9\text{Be} + d \rightarrow {}^{10}\text{B} + n$) with a 3-MeV deuteron beam. The neutron flux at 10 cm on the deuteron-beam axis from the Be target is $(4.9 \pm 1.5) \text{ MHz/cm}^2$ per $1 \mu\text{A}$ of deuteron-beam current. The number of neutrons on the beam axis is inversely proportional to the square of the distance from the target and also depends on the angle relative to the beam axis. This configuration provides an energy spectrum of neutrons with a peak at 2 MeV and fast neutrons below about 9 MeV.

B. Measurement device & Data acquisition

We investigated thermal-neutron-caused SEUs in an Artix-7 (XC7A200T-2FBG676C), which is a 28-nm CMOS process FPGA produced by AMD Inc. The irradiated electronics board with Artix-7 shown in Fig. 1 is called ROESTI. This board has been developed for reading out signals from the straw detector in the COMET experiment [8]. To detect SEUs, we developed firmware applying the Soft Error Mitigation (SEM) Controller [9] provided by AMD Inc., which has a scheme to automatically detect and repair SEUs in the configuration memory of an FPGA. The number of SEUs is recorded in the FPGA register and read by the Personal Computer (PC) every second. There are errors that cannot be automatically repaired by the SEM module and require firmware overwriting, such as multi-bit errors and network communication failures. We call these errors unrecoverable errors, and when they occur, the device control system automatically reprograms the firmware.

Fig. 2 shows a block diagram of the data acquisition (DAQ) system. We collected the value of the deuteron beam current and the number of SEUs detected in the FPGA. To read out the charge of the irradiated deuterons, a copper wire was connected to the flange insulating the beamline around the Be target. The beam current value was converted to a voltage, and then recorded by a data logger (GRAPHTEC GL840) in a control room. A DAQ & control PC was connected to ROESTI as shown in the diagram, it read the number of SEUs and reprogrammed the firmware as the device control system. This PC was placed in a location unaffected by neutron beams and connected to a monitor PC in the control room via the network.

C. Measurement setup

To investigate errors caused by thermal neutrons, we placed the FPGA surrounded by PE blocks or boron-containing PE

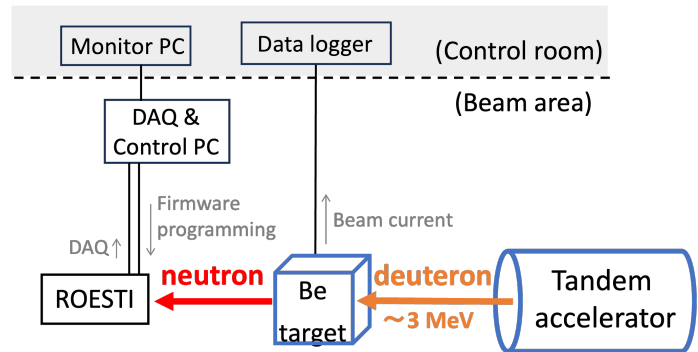


Fig. 2. A block diagram of the data acquisition system

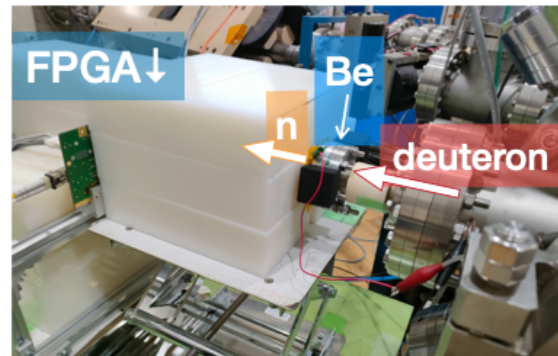


Fig. 3. Photograph of Setting B. The electronics board was placed among the blocks, and the FPGA was positioned off the beam axis. The deuteron beam hits the Be target from the front and a neutron beam is generated

blocks as shown in Fig. 3. ROESTI was placed 22.3 cm from the Be target, and the FPGA was placed 3.9 cm off the deuteron-beam axis. The size of these blocks was $20 \times 10 \times 5 \text{ cm}^3$, and arranged in three vertical layers around the deuteron-beam axis, and behind the FPGA. This setup avoided the neutron beam directly hitting the FPGA, and efficiently irradiated with thermal neutrons through the beam degradation or reflection. When using boron-containing blocks, we can also shield against thermal neutrons. The schematic views of the setups are explained with a bird's eye views in Fig. 4. We built four different setups as follows:

- (A) is a reference. FPGA was directly irradiated neutron beams without any blocks.
- In (B), PE blocks were placed around the beam axis and behind the FPGA to irradiate thermal neutrons by degrading or reflecting fast neutrons.
- In (C), PE blocks containing 10% B_2O_3 were placed in the same positions as in (B) in order to shield both fast and thermal neutrons.
- In (D), we removed the blocks behind the FPGA from the setup (B) and checked the fluence of thermal neutrons generated by the reflection of these blocks.

D. Fluence measurements for fast and thermal neutrons

In order to measure fluences of fast and thermal neutrons, we used CR39, which is a plastic consisting of $\text{C}_{12}\text{H}_{18}\text{O}_7$. It is an abbreviation for Columbia Resin #39 developed by the

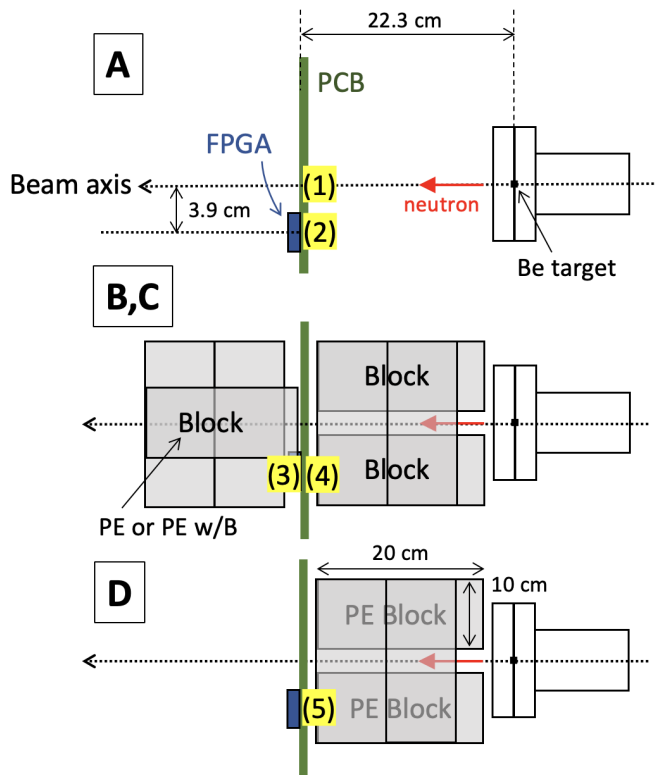


Fig. 4. Four settings in a bird's-eye view. (A) For reference, the neutron beam was directly irradiated. (B) To shield fast neutrons and turn them into thermal neutrons, we put PE blocks. (C) To shield both fast and thermal neutrons, we put PE blocks containing 10% B_2O_3 . (D) To confirm thermal neutrons due to reflection, we removed downstream blocks. The numbers indicate the locations where CR39s were placed.

Columbia Chemical Division, as well as the name of a plastic plate track detector that utilizes this material. CR39 can detect fast or thermal neutrons, respectively, by combining a proton radiator and an alpha particle converter. The measurement energy range of the CR39 used in this study is 0.025 eV - 0.5 eV for thermal neutrons and 24 keV - 15 MeV for fast neutrons, and the measurement dose range is 0.1 mSv - 6 mSv for thermal neutrons and 0.1 mSv - 50 mSv for fast neutrons [10]. We measured neutron fluences by placing the detectors in five different conditions. In Fig. 4, each number corresponds to the locations where the CR39s were placed:

- (1) the location on the beam axis in setup (A);
- (2) the location of the FPGA in setup (A);
- (3) the location of the FPGA in setup (B);
- (4) the location of the FPGA in setup (C);
- (5) the location of the FPGA in setup (D).

The location (1) was for checking the fluences of neutrons coming directly from the beam, and the locations (2), (3), and (4) were for the measurement of fluences of fast and thermal neutrons irradiated on the FPGA in each setup. The location (5) was to see how the backside block, which was placed to reflect fast neutrons, affected the thermal-neutron fluence. Measurements were taken twice, in September and

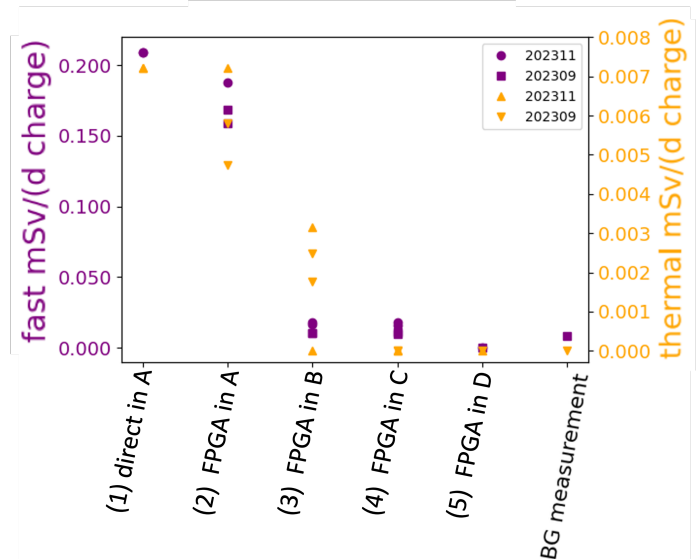


Fig. 5. The measurement results by CR39. The vertical axis represents the effective dose (mSv) of fast and thermal neutrons divided by the deuteron-beam charge. The purple marker is the fast-neutron dose and corresponds to the left vertical axis, and the orange marker corresponds to the right vertical axis. The purple square and the orange lower triangle are the results of the September measurement, and the purple circle and the orange upper triangle are the results of the November measurement.

November 2023. We irradiated CR39s with neutrons for 1, 3, or 5 minutes in each setup and recorded irradiated beam current. The duration of measurement at the location (1) was set to one minute only because direct beam exposure quickly reaches the measurement limit. In the measurement at the location (5), the duration of irradiation was three minutes. For the other locations, the durations of irradiation were set to three patterns.

III. RESULT

A. CR39

The measurement results by CR39 are shown in Fig. 5. Each number on the horizontal axis corresponds to the location described in Fig.4. The left and right vertical axes represent the dose of fast and thermal neutrons measured by CR39s, divided by the beam charge. This normalization allows us to estimate the fluences of fast or thermal neutrons from the beam current in each setup. In the plot, the measurements taken in September are labeled as 202309, with fast neutrons represented by purple squares and thermal neutrons by orange downward triangles. The measurements taken in November are labeled as 202311, with fast neutrons represented by purple circles and thermal neutrons by orange upward triangles. One of the two results of 202311 in the location (3) had thermal-neutron doses below the detection limit of 0.1 mSv. This measurement had only one minute of exposure so it was not statistically enough. In addition, by comparing the difference in the mean of thermal-neutron doses at the location (3) between 202309 and 202311, it can be estimated that the error due to the setup and CR39 resolution is about 30%.

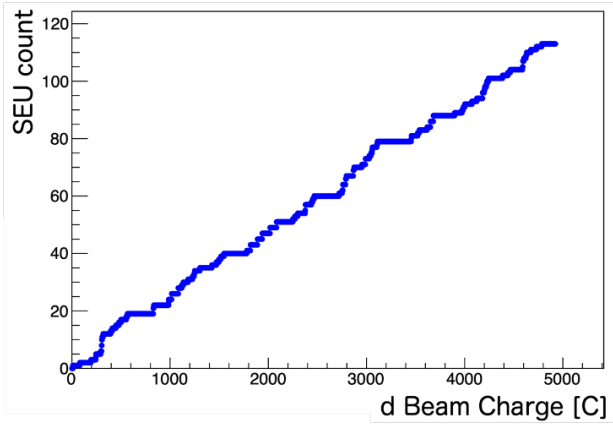


Fig. 6. Deuteron beam charge vs the number of SEU counts in setup (A)

TABLE I

SEU COUNTS, TOTAL DEUTERON BEAM CHARGE, AND THE SEU RATE TO BEAM CHARGE

Setup	SEU count	deuteron charge[C]	SEU / (d charge)
A	113	4.9×10^3	2.3×10^{-2}
B	104	6.2×10^3	1.7×10^{-2}
C	6	4.0×10^3	1.5×10^{-3}

B. SEU

Fig. 6 shows the relationship between the SEUs detected by the SEM module and the total irradiated beam charge in the measurement of setup (A). As seen in this figure, the SEUs increase linearly with the beam charge, i.e. the neutron fluence. Similar proportional trends were observed in the other setups as well. We confirmed that the SEM module was successfully detecting and correcting SEUs during irradiations. Table I lists the results of the SEU measurements. This table displays the counts of SEUs, the total deuteron-beam charge, and the rate of SEUs per beam charge in each setup.

IV. DISCUSSION

From the measurement results by CR39, we consider the energy bands of neutrons irradiated to the FPGA in each setup. The neutron doses at the locations (1) and (2) consisted of both fast and thermal neutrons due to the absence of shields. Comparing (3) and (4), both fast and thermal neutrons were shielded in (4), while only fast neutrons were reduced in (3). This is attributed to the effect of the PE block containing B_2O_3 . Comparing (3) and (5), both setups utilized PE blocks, but the amount of thermal neutrons in (5), which excludes the block behind the FPGA, was significantly reduced. This indicates that the reflection from the blocks behind generated most of the thermal neutrons irradiated at the location (3). These results show the trends in neutron energy at the location of the irradiated FPGA for each setup; (A) has both fast and thermal neutrons, (B) has only thermal neutrons, and (C) has few of both. For further discussion, Fig. 7 plots the ratios of SEUs per beam charge divided by that of setup (A). By normalizing with the result of (A), the error in the neutron beam flux is canceled. The displayed errors arise from a

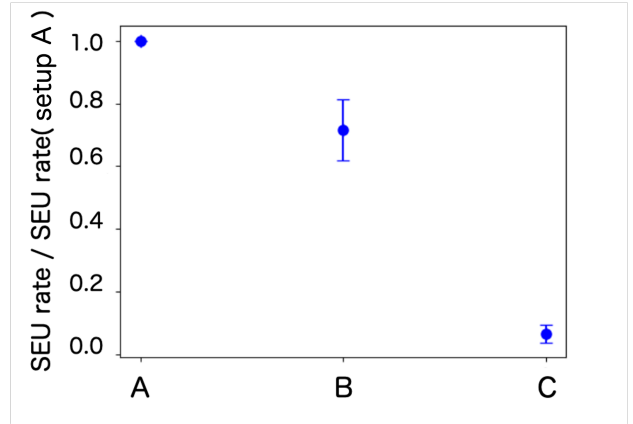


Fig. 7. The ratio of SEU counts per deuteron beam charge to that of setup A

statistical assumption, assuming a Poisson distribution for SEU counting. The results of the measurements of CR39s indicate that fast neutrons were equally shielded in setups (B) and (C), and that only setup (B) was irradiated with thermal neutrons. Considering this, the difference in SEU rates between setups (B) and (C) can be attributed to the presence of thermal neutrons in setup (B). Compared to the SEU rate in setup (A), the decrease in SEU rate in setup (B) was about 70%, indicating that shielding only fast neutrons was not sufficient. On the other hand, the SEU rate in setup (C), where both fast and thermal neutrons were shielded, drops to about 5%. These results indicate that thermal neutrons cause SEUs in the FPGA used in this experiment, and that shielding both thermal and fast neutrons was effective in preventing SEUs.

V. CONCLUSION

SEUs induced by thermal neutrons were investigated using Artix-7, a 28-nm CMOS process FPGA produced by AMD Inc. Fast neutrons, generated by a tandem accelerator, were degraded using polyethylene blocks to become thermal neutrons. These were successfully irradiated onto the FPGA, resulting in observed SEUs caused by thermal neutrons. Furthermore, shielding with boron-containing polyethylene blocks effectively reduced the number of SEUs. These results show thermal neutrons cause SEUs in the FPGA used in our particle physics experiment, and suggest that the use of boron-containing shields is effective in protecting FPGAs in the neutron-rich experimental environment.

ACKNOWLEDGMENT

The authors would like to express their sincere thanks to the staffs of The Tandem Accelerator Laboratory of Kobe University.

REFERENCES

- [1] G. Adamov, *et al.*, "COMET Phase-I Technical Design Report", *Prog. Theor. Exp. Phys* vol.2020, Issue 3, March 2020, 033C01 doi:10.1093/ptep/ptz125
- [2] T. Abe, *et al.*, "Belle II Technical Design Report", *arXiv* 2010. doi:arXiv:1011.0352

- [3] T. H. Tetsuo INADA, Kiyomitsu KAWACHI, "Neutrons from Thick Target Beryllium (d,n) Reactions at 1.0 MeV to 3.0 MeV", *J. Nucl. Sci. Technol.* vol. 5, no. 22, pp. 22-29, Jan 1968, <https://doi.org/10.3327/jnst.5.22>
- [4] Y. Nakazawa, *et al.*, "Radiation study of FPGAs with neutron beam for COMET phase-I", *Nucl. Instrum. Methods A*, vol. 936, no. 21, August 2019, pp.351-352 doi.org/10.1016/j.nima.2018.10.130.
- [5] Yutaka Arita Yutaka Arita *et al.*"Experimental Investigation of Thermal Neutron-Induced Single Event Upset in Static Random Access Memories" 2001 Jpn. J. Appl. Phys. 40 L151
- [6] H. Iwashita *et al.*, "Energy-Resolved SEU Cross Section From 10-meV to 800-MeV Neutrons by Time-of-Flight Measurement," *IEEE Trans. Nucl. Sci.*, vol. 70, no. 3, pp. 216-221, March 2023, doi: 10.1109/TNS.2023.3245142.
- [7] Andrea Coronetti, *et al.* "Thermal-to-high-energy neutron SEU characterization of commercial SRAMs" *IEEE Radiation Effects Data Workshop (REDW), Ottawa, ON, Canada, 2021*, pp. 1-5, doi: 10.1109/NSREC45046.2021.9679344
- [8] K.Ueno, *et al.* "Design and performance evaluation of front-end electronics for COMET straw tracker",*Nucl. Instrum. Methods A*, vol. 936, no. 2019, pp. 297-299, doi:10.1016/j.nima.2018.08.027
- [9] *Soft Error Mitigation Controller v4.1 LogiCORE IP Product Guide*, AMD PG036
- [10] *Luminescence Badge (for Neutron Beam) Catalog*, Nagase Landauer K.K.